Non-coding RNA Research 9 (2024) 1342–1350

Contents lists available at ScienceDirect

Non-coding RNA Research

journal homepage: www.keaipublishing.com/en/journals/non-coding-rna-research

Original Research Article

Plasma microRNA-15a/16-1 serves as a non-invasive indicator of liver fibrosis severity in individuals with chronic hepatitis B

Huan Wei [a,1], Yanhua Bi [a,b,1], Chunhong Liao [a], Yuehua Huang [a,c,*], Yifan Lian [a,**]

[a] Guangdong Provincial Key Laboratory of Liver Disease Research, The Third Affiliated Hospital of Sun Yat-sen University, Guangzhou, China
[b] School of Public Health, Sun Yat-sen University, Guangzhou, China
[c] Department of Infectious Diseases, The Third Affiliated Hospital of Sun Yat-sen University, Guangzhou, China

ARTICLE INFO

Keywords:
microRNA-15a
microRNA-16-1
Biomarker
Liver fibrosis
Cirrhosis
Chronic hepatitis B (CHB)

ABSTRACT

Background: The lack of effective non-invasive diagnostic methods for liver fibrosis hinders timely treatment for chronic hepatitis B (CHB) patients, leading to the progression of advanced liver disease. Circulating microRNAs offer a non-invasive approach to fibrosis assessment. MicroRNA-15a/16-1 (miR-15a/16) was reported to be implicated in fibrosis development, but the role of plasma miR-15a/16 in liver fibrosis assessment remains poorly understood. This study explored the importance of plasma miR-15a/16 in assessing liver fibrosis severity of CHB patients.

Methods: Quantitative PCR was utilized to measure the levels of plasma miR-15a/16 in 435 patients with CHB and 74 healthy controls. We assessed the correlation between plasma miR-15a/16 levels and liver fibrosis and cirrhosis using Pearson correlation coefficients, multivariate linear and logistic regression models, and smooth curve fitting. Utilizing the receiver operating characteristic (ROC) curve, we examined the diagnostic potential of plasma miR-15a/16 in severe fibrosis and cirrhosis.

Results: Plasma levels of miR-15a/16 in patients with CHB were significantly reduced compared to those in healthy controls. In the CHB cohort, levels were notably decreased in individuals with severe fibrosis or cirrhosis compared to those without severe fibrosis or cirrhosis. Plasma miR-15a/16 levels exhibited a negative relationship with the severity of liver fibrosis, gradually decreasing as the histological fibrosis stage progressed from S0 to S4. Reduced levels of plasma miR-15a/16 were linked to an elevated risk of severe liver fibrosis (miR-15a: odds ratio [OR] = 0.243; 95 % confidence interval [CI]: 0.138, 0.427; miR-16: OR = 0.201; 95 % CI: 0.097, 0.417) and cirrhosis (miR-15a: OR = 0.153; 95 % CI: 0.079, 0.298; miR-16: OR = 0.064; 95 % CI: 0.025, 0.162). MiR-15a achieved an area under the ROC curve of 0.886 and 0.832 for detecting moderate-to-severe fibrosis (S2-S4) and cirrhosis, respectively. MiR-16 demonstrated similar diagnostic values.

Conclusion: Plasma miR-15a/16 levels were negatively correlated with the severity of liver fibrosis in CHB patients and could serve as a new non-invasive indicator in evaluating liver fibrosis.

1. Introduction

Liver fibrosis, a progressive condition, can advance to cirrhosis and ultimately lead to hepatocellular carcinoma (HCC), substantially augmenting the global disease burden [1]. Chronic inflammation and hepatic injury resulting from persistent infection with hepatitis B virus (HBV) are substantial risk factors for liver fibrosis [2]. Therefore, assessing hepatic fibrosis in individuals with chronic hepatitis B (CHB) is important for identifying patients prone to cirrhosis. Furthermore, the assessment of liver fibrosis in CHB patients is recommended by the American Association for the Study of Liver Diseases guidelines (2018) [3].

Liver biopsy remains the gold standard for evaluating liver fibrosis. However, its application is currently limited due to invasiveness [1].

* Corresponding author. Guangdong Provincial Key Laboratory of Liver Disease Research and Department of Infectious Diseases, The Third Affiliated Hospital of Sun Yat-sen University, China.
** Corresponding author. Guangdong Provincial Key Laboratory of Liver Disease Research, The Third Affiliated Hospital of Sun Yat-sen University, Guangzhou, China.
E-mail addresses: huangyh53@mail.sysu.edu.cn (Y. Huang), lianyf6@mail.sysu.edu.cn (Y. Lian).
[1] Tow authors contributed equally.

https://doi.org/10.1016/j.ncrna.2024.08.004
Received 21 June 2024; Received in revised form 5 August 2024; Accepted 14 August 2024
Available online 15 August 2024

Table 1
Clinical features of the participants.

Variables	HC	CHB		*P* value
	(n = 74)	Non-cirrhosis (n = 256)	Cirrhosis (n = 179)	
Gender				
Female	23.0 (31.1 %)	59.0 (23.0 %)	35.0 (19.6 %)	0.140
Male	51.0 (68.9 %)	197.0 (77.0 %)	144.0 (80.4 %)	
Age (years)	42.8 ± 10.9	41.8 ± 10.5	51.6 ± 8.9	<0.001
AST (U/L)	20.2 ± 4.0	86.7 ± 234.0	68.0 ± 100.9	0.314
ALT (U/L)	19.1 ± 6.4	127.4 ± 338.0	58.7 ± 79.4	0.008
ALB (g/L)	NA	45.2 ± 4.2	38.7 ± 7.5	<0.001
AGR	NA	1.6 ± 0.3	1.3 ± 0.4	<0.001
TBIL (umol/L)	NA	28.1 ± 64.1	41.7 ± 84.6	0.057
WBC (× 10^9/L)	NA	6.0 ± 2.0	5.2 ± 2.3	<0.001
PLT (× 10^9/L)	NA	203.8 ± 75.4	109.6 ± 59.4	<0.001
HBV-DNA (IU/mL)	NA	(1.6E + 07) ± (4.5E + 07)	(2.1E + 06) ± (1.4E + 07)	<0.001
Inflammation grades (G0/G1/G2/G3/G4/NA)	NA	(3/12/13/2/0/226)	(0/0/2/1/0/176)	NA
Fibrosis stages (S0/S1/S2/S3/S4/NA)	NA	(6/11/9/4/0/226)	(0/0/0/0/3/176)	NA

Data are mean ± standard deviation or n (percentages). The *P*-values for the difference between non-cirrhosis and cirrhosis groups in CHB cohorts. HC, healthy control; CHB, chronic hepatitis B; AST, aspartate aminotransferase; ALT, alanine aminotransferase; ALB, albumin; AGR, albumin to globulin ratio; TBIL, total bilirubin; WBC, white blood cells; PLT, platelet; HBV-DNA, hepatitis B virus deoxyribonucleic acid; NA, not available.

Moreover, liver biopsy samples only a minute portion of the entire organ, potentially lacking a comprehensive representation of hepatic fibrosis due to the heterogeneous distribution of fibrotic lesions [4]. Ultrasonography and standard liver biochemistry are not recommended for assessing liver fibrosis because of their low sensitivity and specificity [5,6]. Transient elastography, a technique that measures liver stiffness, has shown good accuracy in evaluating fibrosis and cirrhosis [7]. However, the accuracy of transient elastography may be influenced by factors such as inflammation, biliary obstruction, and hepatic congestion in patients [7,8]. While magnetic resonance imaging (MRI) techniques may offer superior efficacy in hepatic fibrosis assessment compared to the tests mentioned above, they are characterized by higher costs and limited accessibility [9]. Therefore, improvements in liver fibrosis evaluation, especially in identifying reliable non-invasive diagnostic biomarkers, are urgently needed.

MicroRNAs (miRNAs), short non-coding RNAs about 22 nucleotides long, are involved in numerous biological processes [10]. MiRNA-15a/16-1 (miR-15a/16) is a cluster of miRNA located in the 13q14 chromosomal area in humans [11]. Our previous study found that HBV infection inhibited the miR-15a/16 expression in HCC cells [12]. Consistently, several studies have also demonstrated that the transcripts and proteins of HBV downregulate the expression of miR-15a/16 in hepatocytes in vitro [13,14]. Furthermore, dysregulation of miR-15a/16 is associated with the activation and proliferation of hepatic stellate cells (HSC), contributing to fibrosis [15–17]. These findings indicated their significant role in the initiation and advancement of liver fibrosis. However, the relationship between plasma miR-15a/16 and liver fibrosis remains unclear. Given that circulating miRNAs can be stably detected in human peripheral blood and have reproducible concentrations among individuals [18], and coupled with our previous demonstration of plasma miR-15a/16 as a biomarker for HBV-related HCC [19], we aimed to investigate whether plasma miR-15a/16 could also potentially serve as a biomarker for assessing liver fibrosis in individuals with CHB. Thus, in this study, we explored the association between plasma miR-15a/16 and liver fibrosis, severe liver fibrosis, and cirrhosis in CHB patients using a large clinical cohort. Furthermore, we evaluated the potential of plasma miR-15a/16 as a circulating indicator for assessing liver fibrosis.

2. Materials and methods

2.1. Participants

Between May 2021 and December 2023, we enrolled 509 participants from The Third Affiliated Hospital of Sun Yat-sen University, comprising 74 healthy controls (HC) and 435 individuals with chronic hepatitis B (CHB). The inclusion criteria were adults aged 18 to 90, both men and women. Healthy controls were required to be in good health with no liver or systemic ailments, while CHB patients needed to test positive for hepatitis B surface antigen for over 6 months [3]. The exclusion criteria for all groups included prior or ongoing infection with hepatitis viruses other than HBV and the presence of non-HBV-related systemic disorders.

During the first visit, data on the medical history and test results of every patient were gathered from the record system. The histological liver fibrosis stage (S0-S4) and inflammation grade (G0-G4) of the patients were confirmed by two independent pathologists. We also defined severe liver fibrosis using either the aspartate aminotransferase (AST) to platelet (PLT) ratio index (APRI) [20] or the fibrosis index based on four factors (FIB-4), which includes age, AST, alanine aminotransferase (ALT), and PLT [21]. Calculation of FIB-4 and APRI scores followed established methodologies as previously described [20,21]. Severe liver fibrosis was categorized as an APRI score ≥1.5 or a FIB-4 score ≥3.25 [20,21]. The diagnosis of cirrhosis relied on either biopsy or the concurrence of two imaging examinations (ultrasound coupled with computed tomography and/or MRI) [22].

We received informed consent from all participants, and the study was approved by the Institute Research Ethics Committee of The Third Affiliated Hospital of Sun Yat-sen University (Ethical approval No. [2021] 02-274-01).

2.2. Plasma sample collection

We drew 5 mL of peripheral blood from all participants into tubes containing ethylenediaminetetraacetic acid for plasma collection. Within half an hour, the blood was centrifuged at 4 °C for 10 min at 1000 g. The supernatant was then subjected to a second centrifugation at 4 °C for 10 min at 1000 g to remove residual cellular debris. Finally, we aliquoted the resultant supernatant into 200 μL portions and stored it at −80 °C until further use.

2.3. Plasma RNA extraction

We used TRIzol reagent (Invitrogen Carlsbad, USA) to extract total RNA, including microRNA, from 200 μL of plasma. Before isolating RNA, synthetic *cel*-miR-39-3p (RiboBio, Guangzhou, China) from *Caenorhabditis elegans* was added to the plasma samples at a concentration of 0.2 nM to serve as a reference. We also added glycogen (Ambion/Applied Biosystems, Foster City, CA, USA) to aid RNA precipitation, with a final concentration of 100 μg/mL during isopropanol precipitation. Afterward, the RNA pellet was air-dried at room temperature and redissolved with 10 μL of RNase-free water.

2.4. MiRNA quantitation by real-time quantitative PCR

Plasma miRNA levels were measured using real-time quantitative PCR (RT-qPCR). Briefly, the extracted plasma RNA underwent poly(A) tailing and reverse transcription into complementary DNA using

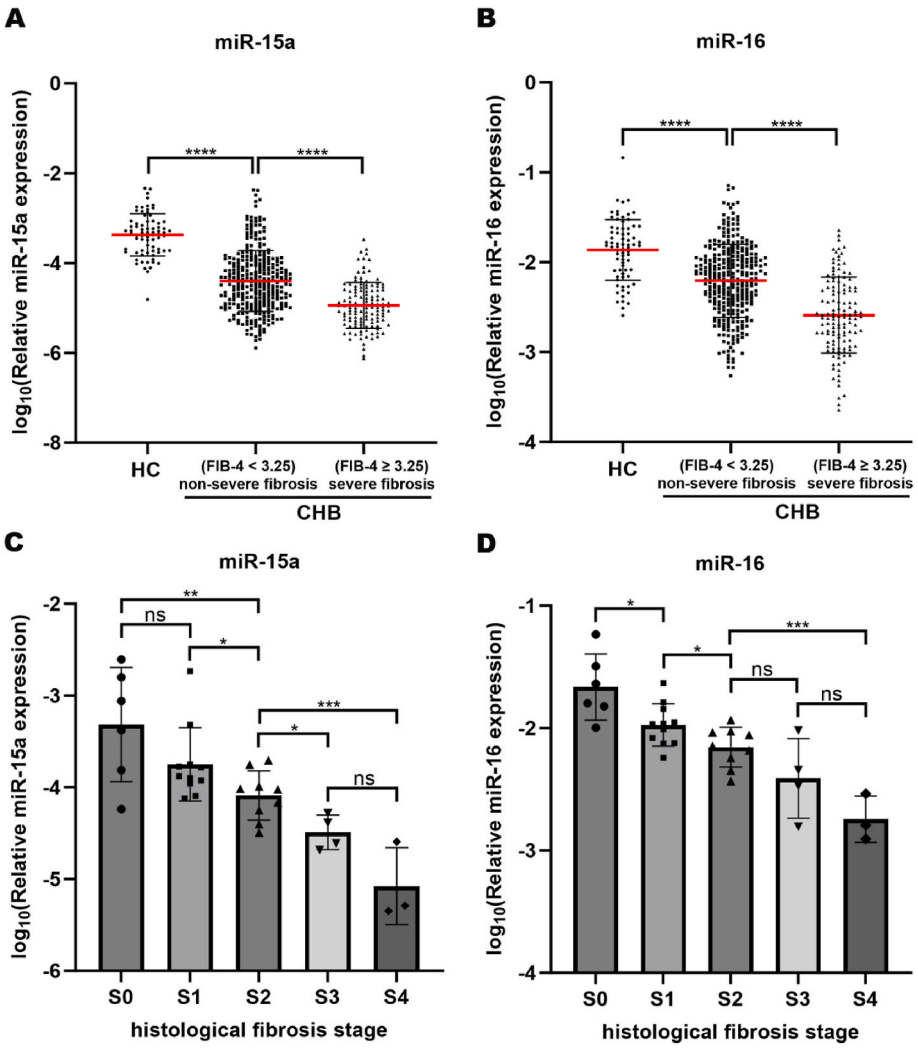

Fig. 1. Plasma levels of miR-15a/16 in CHB patients with different fibrosis stages. Plasma miR-15a (A) and miR-16 (B) levels of HC and CHB, where CHB were classified into non-severe fibrosis (FIB-4 < 3.25) and severe fibrosis (FIB-4 ≥ 3.25). Plasma levels of miR-15a (C) and miR-16 (D) in individual histological liver fibrosis stages (S0-S4) of CHB patients. *$P < 0.05$, **$P < 0.01$, ***$P < 0.001$, ****$P < 0.0001$; ns, not significant. HC, healthy controls. CHB, chronic hepatitis B. FIB-4, fibrosis index based on four factors (incorporating age, aspartate aminotransferase, alanine aminotransferase, and platelet).

Escherichia coli poly(A) polymerase (New England Biolabs, Ipswich, MA, USA) and the GoScript™ Reverse Transcription System (Promega, Madison, USA), respectively. Platinum SYBR Green qPCR SuperMix-UDG (Invitrogen, Grand Island, USA) was used for RT-qPCR analysis of miR-15a/16 levels on a LightCycler 480 system (Roche, Indianapolis, USA). Primer sequences for miRNA RT-qPCR amplification were designed as previously described [23], with details provided in Supplementary Table 1. The primers of this investigation were purchased from RuiBiotech in Beijing, China. The levels of plasma miRNA were standardized to *cel*-miR-39 and calculated using the $2^{-\Delta Ct}$ method, with ΔCt being defined as the value of Ct_{target} minus $Ct_{reference}$.

2.5. Statistical analysis

Statistical analyses were performed using software of SPSS 26.0 (IBM Inc., Chicago, IL, USA), GraphPad Prism 9.0 (San Diego, CA, USA), R (version 4.0.2; http://www.R-project.org), and EmpowerStats (https://www.empowerstats.net/en/). Statistical tests were conducted as two-sided, with *P*-values below 0.05 considered statistically significant. We presented continuous variables as mean ± standard deviation, while categorical variables were shown as the number of cases with corresponding percentages. Contingency tables were used for categorical variables, and the chi-square test was employed to assess distribution variability among clinical indicators. Continuous variables were analyzed using Student's t-test to compare means between two groups. Pearson's correlation coefficient was used to assess the linear correlation between two variables. To investigate the correlation between plasma miR-15a/16-1 levels and liver fibrosis, we stratified CHB patients into four distinct groups based on the quartiles of their miR-15a or miR-16-1 plasma levels. The first group, quartile 1 (Q1), comprised patients with miR-15a/16-1 levels below the lower quartile. The second group, quartile 2 (Q2), included those with levels between the lower quartile and the median. The third group, quartile 3 (Q3), consisted of patients with levels between the median and the upper quartile. Finally, the fourth group, quartile 4 (Q4), encompassed patients with miR-15a/16-1 levels above the upper quartile. Furthermore, multivariable linear and multivariable logistic regression models were constructed to investigate the correlation of plasma miR-15a/16 with liver fibrosis, severe liver fibrosis, or cirrhosis. We performed smooth curve fitting to address nonlinearity associations. The diagnostic efficacy of plasma miR-15a/16 was analyzed using receiver operating characteristic (ROC) curves.

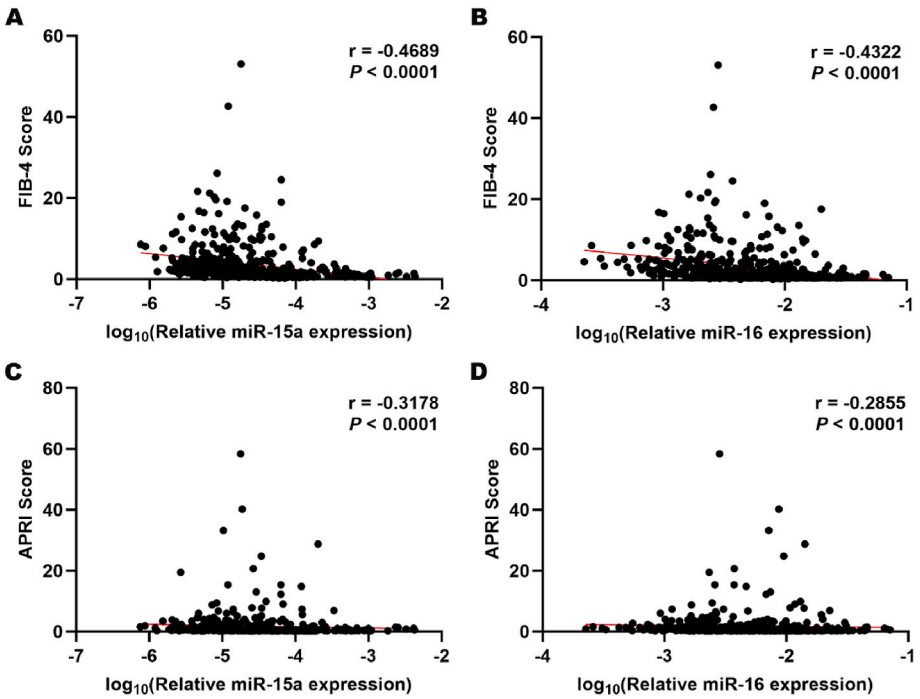

Fig. 2. Association between plasma levels of miR-15a/16 and liver fibrosis (FIB-4 and APRI) in CHB patients by Pearson's correlation analysis. Plasma levels of miR-15a (A) and miR-16 (B) exhibited a negative correlation with FIB-4. Plasma levels of miR-15a (C) and miR-16 (D) exhibited a negative correlation with APRI. FIB-4, fibrosis index based on four factors (incorporating age, aspartate aminotransferase, alanine aminotransferase, and platelet). APRI, aspartate aminotransferase to platelet ratio index. CHB, chronic hepatitis B.

3. Results

3.1. Clinical features of the participants

In Table 1, we display the clinical characteristics of participants by subgroup. Our cohort comprised 435 CHB patients and 74 healthy controls. Of the CHB patients, 179 (41.1 %) had cirrhosis, while the remaining 256 (58.9 %) did not. There were no significant differences in gender distribution or the mean levels of AST and total bilirubin (TBIL) between the cirrhosis and non-cirrhosis groups. Compared to the non-cirrhosis cohort, the cirrhosis group exhibited higher age and HBV-DNA levels, alongside lower levels of ALT, albumin (ALB), albumin to globulin ratio (AGR), white blood cells (WBC), and PLT.

3.2. Plasma miR-15a/16 levels in CHB patients with different fibrosis stages

We first compared plasma miR-15a/16 levels between CHB patients and healthy controls. The results showed that plasma miR-15a/16 levels were significantly lower in CHB patients than in healthy controls ($P < 0.0001$ for all, Fig. 1A and B). We then investigated whether miR-15a/16 plasma levels differed by fibrosis stage. We observed that plasma levels of miR-15a/16 gradually decreased as the histological fibrosis stage progressed from S0 to S4 (Fig. 1C and D). Plasma miR-15a/16 levels were also significantly lower in inflammation grades G2-G3 compared to G0-G1 (Supplementary Fig. 1A and B, $P < 0.01$ for all). Furthermore, patients with severe liver fibrosis had significantly lower plasma miR-15a/16 levels compared to those without severe liver fibrosis when stratified by FIB-4 ($P < 0.0001$ for all; Fig. 1A and B) or APRI ($P < 0.01$ for all, Supplementary Figs. 2A and B). Additionally, compared with non-cirrhosis patients, those with cirrhosis exhibited significantly reduced plasma miR-15a/16 levels. ($P < 0.0001$ for all; Supplementary Figs. 2C and D).

3.3. Association between plasma miR-15a/16 levels and severity of liver fibrosis

Simple linear correlation analysis showed moderately significant negative associations between plasma miR-15a/16 levels and FIB-4 scores (Fig. 2A and B), and weak but significant negative correlations between plasma miR-15a/16 levels and APRI scores (Fig. 2C and D). Subsequently, multivariate linear regression analysis was conducted to explore the relationship between miR-15a/16 and liver fibrosis. We performed three distinct models to assess the beta (β) coefficient values (95 % CI) of miR-15a/16. The variables used to calculate FIB-4 or APRI scores were not adjusted in the corresponding models. Therefore, for the three models of FIB-4: model 1, without any covariate adjustments; model 2, adjusted for gender; model 3, gender, ALB, AGR, TBIL, WBC, and HBV-DNA were adjusted. For the three models of APRI: model 1, without any covariate adjustments; model 2, adjusted for gender and age; model 3, gender, age, ALT, ALB, AGR, TBIL, WBC, and HBV-DNA were adjusted.

As shown in Table 2, the results indicated that miR-15a was significantly negatively associated with FIB-4 in all the multivariate linear regression models. Specifically, in model 1, the beta coefficient was −0.259 (95 % CI: 2.623, −1.255); in model 2, the beta coefficient was −0.258 (95 % CI: 2.622, −1.255); and in model 3, the association persisted with a slightly reduced beta coefficient of −0.135 (95 % CI: 1.579, −0.443). The strength of this association increased progressively from the lowest quartile group (Q1) to the highest quartile group (Q4) of miR-15a (P for trend <0.001). Similarly, significant negative associations and trends were observed between miR-16 and FIB-4 in models 1 and 2. The beta coefficient in model 1 was −0.257 (95 % CI: 3.971, −1.887). In model 2, the beta coefficient was −0.252 (95 % CI: 3.927, −1.835). However, this association was not observed in model 3, where the beta coefficient was −0.068 (95 % CI: 1.650, 0.102). Upon conducting subgroup analysis by gender, negative correlations between miR-15a/16 and FIB-4 persisted across all models in males. However, in females, significant correlations were only found in model 1. On the other hand,

Table 2
Analysis of the correlation between plasma miR-15a/16 and liver fibrosis (FIB-4) in CHB patients by multivariate linear regression.

Variables	Model 1 β (95 % CI) *P* value (n = 435)	Model 2 β (95 % CI) *P* value (n = 435)	Model 3 β (95 % CI) *P* value (n = 435)
miR-15a	−0.259 (−2.623, −1.255) 4.5E-08	−0.258 (−2.622, −1.255) 4.4E-08	−0.135 (−1.579, −0.443) 0.0005
Quartile groups of miR-15a			
Q1	Reference	Reference	Reference
Q2	−0.077 (−2.217, 0.400) 0.1730	−0.075 (−2.191, 0.421) 0.1840	−0.055 (−1.656, 0.374) 0.2153
Q3	−0.188 (−3.508, −0.898) 0.0010	−0.184 (−1.732, −0.429) 0.0012	−0.126 (−2.514, −0.432) 0.0057
Q4	−0.319 (−5.048, −2.438) 3.1E-08	−0.321 (−1.688, −0.819) 2.6E-08	−0.166 (−3.033, −0.864) 0.0005
P for trend	4.9E-09	4.3E-09	0.0002
miR-16	−0.257 (−3.971, −1.887) 5.7E-08	−0.252 (−3.927, −1.835) 1.0E-07	−0.068 (−1.650, 0.102) 0.0831
Quartile groups of miR-16			
Q1	Reference	Reference	Reference
Q2	0.001 (−1.311, 1.323) 0.9929	0.009 (−1.215, 1.431) 0.8724	0.018 (−0.834, 1.265) 0.6866
Q3	−0.184 (−3.474, −0.846) 0.0013	−0.181 (−3.436, −0.810) 0.0016	−0.035 (−1.469, 0.660) 0.4554
Q4	−0.248 (−4.221, −1.593) 1.7E-05	−0.241 (−4.143, −1.508) 3.0E-05	−0.043 (−1.600, 0.583) 0.3610
P for trend	4.2E-07	6.3E-07	0.2221
Stratified by gender[a]			
miR-15a			
Female	−0.241 (−4.129, −0.375) 0.0192	NA[a]	−0.086 (−2.035, 0.420) 0.1946
Male	−0.271 (−2.536, −1.141) 3.8E-07	NA[a]	−0.154 (−1.643, −0.445) 0.0007
miR-16			
Female	−0.216 (−6.227, −0.206) 0.0365	NA[a]	0.033 (−1.485, 2.481) 0.6187
Male	−0.272 (−3.838, −1.734) 3.3E-07	NA[a]	−0.098 (−1.909, −0.089) 0.0316

Model 1: without any covariate adjustments. Model 2: adjusted for gender. Model 3: gender, albumin, albumin to globulin ratio, total bilirubin, white blood cells, and hepatitis B virus DNA were adjusted.
CHB, chronic hepatitis B; FIB-4, fibrosis index based on four factors (incorporating age, aspartate aminotransferase, alanine aminotransferase, and platelet); CI, confidence intervals; NA, not available.
[a] The models of gender stratification excluded gender as an adjustment variable.

Table 3
Analysis of the correlation between plasma miR-15a/16 and severe liver fibrosis (FIB-4 ≥ 3.25) in CHB patients by multivariate logistic regression.

Variables	Model 1 OR (95 % CI) *P* value (n = 435)	Model 2 OR (95 % CI) *P* value (n = 435)	Model 3 OR (95 % CI) *P* value (n = 435)
miR-15a	0.214 (0.140, 0.328) 1.4E-12	0.213 (0.139, 0.327) 1.4E-12	0.243 (0.138, 0.427) 8.7E-07
Quartile groups of miR-15a			
Q1	Reference	Reference	Reference
Q2	14.897 (6.611, 33.572) 7.2E-11	15.288 (6.761, 34.572) 5.7E-11	11.589 (3.997, 33.601) 6.5E-06
Q3	5.555 (2.427, 12.72) 4.9E-05	5.721 (2.491, 13.14) 3.9E-05	3.407 (1.164, 9.971) 0.0253
Q4	4.157 (1.793, 9.639) 0.0009	4.313 (1.845, 10.036) 0.0007	3.411 (1.135, 10.248) 0.0288
P for trend	1.2E-12	1.4E-07	2.8E-06
miR-16	0.108 (0.061, 0.193) 4.7E-14	0.110 (0.062, 0.196) 7.5E-14	0.201 (0.097, 0.417) 1.6E-05
Quartile groups of miR-16			
Q1	Reference	Reference	Reference
Q2	9.766 (4.717, 20.220) 8.4E-10	9.551 (4.606, 19.803) 1.3E-09	4.218 (1.693, 10.507) 0.0020
Q3	4.643 (2.217, 9.723) 4.7E-05	4.690 (2.237, 9.831) 4.3E-05	2.127 (0.823, 5.459) 0.1166
Q4	2.253 (1.034, 4.911) 0.0411	2.221 (1.018, 4.846) 0.0450	1.828 (0.697, 4.794) 0.2199
P for trend	6.5E-12	9.5E-12	0.0015
Stratified by gender[a]			
miR-15a			
Female	0.204 (0.089, 0.464) 0.0002	NA[a]	0.286 (0.090, 0.905) 0.0333
Male	0.217 (0.131, 0.358) 2.2E-09	NA[a]	0.206 (0.103, 0.411) 7.7E-06
miR-16			
Female	0.076 (0.022, 0.259) 3.9E-05	NA[a]	0.100 (0.014, 0.710) 0.0213
Male	0.124 (0.064, 0.238) 3.9E-10	NA[a]	0.200 (0.088, 0.457) 0.0001

Model 1: without any covariate adjustments. Model 2: adjusted for gender. Model 3: gender, albumin, albumin to globulin ratio, total bilirubin, white blood cells, and hepatitis B virus DNA were adjusted.
FIB-4, fibrosis index based on four factors (incorporating age, aspartate aminotransferase, alanine aminotransferase, and platelet); CHB, chronic hepatitis B; OR, odds ratio; CI, confidence intervals; NA, not available.
[a] The models of gender stratification excluded gender as an adjustment variable.

miR-15a/16 demonstrated no correlations with APRI in multivariable linear analysis (Supplementary Table 2). Furthermore, smooth curve fitting was employed to examine the nonlinear relationship, confirming that miR-15a/16 levels decreased with increasing FIB-4 (Supplementary Figs. 3A–F) and APRI (Supplementary Figs. 4A–F).

3.4. Plasma levels of miR-15a/16 was correlated with the risk of severe liver fibrosis

We performed multivariate logistic regression analysis to further investigate the connection between miR-15a/16 and severe liver fibrosis. In this analysis, we adjusted the same variables as in the three models used in the multivariable analysis of liver fibrosis in section 3.3.

As shown in Table 3 based on FIB-4 stratification, a consistent negative association was found between miR-15a/16 and the prevalence of severe liver fibrosis across all models. For miR-15a, the odds ratios (ORs) were as follows: model 1, 0.214 (95 % CI: 0.140, 0.328); model 2, 0.213 (95 % CI: 0.139, 0.327); model 3, 0.243 (95 % CI: 0.138, 0.427). Similarly, for miR-16, the ORs were: model 1, 0.108 (95 % CI: 0.061, 0.193); model 2, 0.110 (95 % CI: 0.062, 0.196); model 3, 0.201 (95 % CI: 0.097, 0.417). Remarkably, upon comprehensive adjustment for potential confounders in model 3, each unit decrease in miR-15a or miR-16 was associated with a 75.7 % or 79.9 % increased risk of severe liver fibrosis, respectively. Furthermore, a notable decreasing trend in the risk

Table 4
Analysis of the correlation between plasma miR-15a/16 and cirrhosis in CHB patients by multivariate logistic regression.

Variables	Model 1 OR (95 % CI) *P* value (n = 435)	Model 2 OR (95 % CI) *P* value (n = 435)	Model 3 OR (95 % CI) *P* value (n = 435)
miR-15a	0.078 (0.047, 0.131) 6.7E-22	0.098 (0.057, 0.169) 6.2E-17	0.153 (0.079, 0.298) 3.3E-08
Quartile groups of miR-15a			
Q1	Reference	Reference	Reference
Q2	37.333 (16.521, 84.364) 3.2E-18	23.019 (9.884, 53.611) 3.6E-13	9.117 (3.284, 25.313) 2.0E-05
Q3	14.421 (6.604, 31.490) 2.1E-11	9.255 (4.093, 20.929) 9.1E-08	4.869 (1.856, 12.773) 0.0013
Q4	3.307 (1.463, 7.473) 0.0040	2.294 (0.973, 5.406) 0.0577	1.045 (0.356, 3.064) 0.9360
P for trend	4.6E-24	1.6E-17	1.0E-07
miR-16	0.035 (0.018, 0.069) 2.9E-22	0.038 (0.018, 0.080) 6.3E-18	0.064 (0.025, 0.162) 6.2E-09
Quartile groups of miR-16			
Q1	Reference	Reference	Reference
Q2	31.553 (14.602, 68.182) 1.6E-18	27.119 (11.774, 62.459) 9.0E-15	13.989 (4.900, 39.938) 8.3E-07
Q3	7.971 (3.846, 16.521) 2.7E-08	6.226 (2.846, 13.619) 4.7E-06	5.034 (1.853, 13.675) 0.0015
Q4	3.702 (1.754, 7.816) 0.0006	3.482 (1.560, 7.770) 0.0023	3.471 (1.277, 9.435) 0.0147
P for trend	1.2E-21	1.3E-16	3.4E-07
Stratified by gender[a]			
miR-15a			
Female	0.083 (0.028, 0.243) 5.7E-06	0.081 (0.023, 0.280) 7.3E-05	0.240 (0.043, 1.325) 0.1016
Male	0.076 (0.042, 0.138) 1.9E-17	0.102 (0.055, 0.188) 2.4E-13	0.145 (0.069, 0.307) 4.1E-07
miR-16			
Female	0.047 (0.013, 0.178) 6.3E-06	0.041 (0.009, 0.196) 6.0E-05	0.060 (0.004, 1.007) 0.0505
Male	0.028 (0.013, 0.063) 4.3E-18	0.036 (0.016, 0.085) 2.4E-14	0.061 (0.022, 0.170) 8.9E-08

Model 1: without any covariate adjustments. Model 2: adjusted for age and gender. Model 3: age, gender, aspartate aminotransferase, alanine aminotransferase, albumin, albumin to globulin ratio, total bilirubin, white blood cells, platelet count, and hepatitis B virus DNA were adjusted.
CHB, chronic hepatitis B; OR, odds ratio; CI, confidence intervals.
[a] The models of gender stratification excluded gender as an adjustment variable.

of severe liver fibrosis was observed across the increasing quartile groups (Q1-Q4) of miR-15a/16 levels (*P* for trend <0.01). Significant negative associations were also observed in both males and females in all models. According to APRI stratification, similar results were obtained in the three models of miR-15a and in models 1 and 2 of miR-16 and their corresponding male subgroups (Supplementary Table 3). However, in females, a significant negative correlation was found only in model 1 for miR-15a (Supplementary Table 3).

3.5. Plasma levels of miR-15a/16 was correlated with the risk of cirrhosis

We observed a significant reduction in plasma miR-15a/16 levels among cirrhosis patients (Supplementary Figs. 2C and D). Therefore, we performed similar multivariate logistic regression analyses for miR-15a/16 in relation to cirrhosis. As shown in Table 4, miR-15a/16 exhibited a negative correlation with cirrhosis risk across all three models (miR-15a: model 1, OR = 0.078; 95 % CI: 0.047, 0.131; model 2: OR = 0.098; 95 % CI: 0.057, 0.169; model 3: OR = 0.153; 95 % CI: 0.079, 0.298. miR-16: model 1, OR = 0.035; 95 % CI: 0.018, 0.069; model 2: OR = 0.038; 95 % CI: 0.018, 0.080; model 3: OR = 0.064; 95 % CI: 0.025, 0.162). Notably, in model 3, following comprehensive adjustment for potential confounders, each unit decrease in miR-15a or miR-16 was associated with an increased risk of cirrhosis by 84.7 % or 93.6 %, respectively. Furthermore, the risk of cirrhosis gradually decreased with the elevation of miR-15a/16 quartile groups from Q1 to Q4 (*P* for trend <0.0001). Upon stratification by gender, the negative associations between miR-15a/16 and cirrhosis prevalence persisted in both males and females in models 1 and 2. However, in model 3, the negative associations were more significant in males.

3.6. Plasma miR-15a/16 could be a diagnostic indicator for severe liver fibrosis and cirrhosis

We performed ROC cove analysis to assess the diagnostic efficacy of plasma miR-15a/16 for severe liver fibrosis and cirrhosis. The findings show that, in detecting moderate-to-severe fibrosis (S2-S4), miR-15a (area under the curve [AUC] 0.886, sensitivity 87.5 %, and specificity 82.4 %), miR-16 (AUC 0.884, sensitivity 93.8 %, and specificity 76.5 %), and the combined miR-15a and miR-16 (AUC 0.893, sensitivity 75.0 %, and specificity 88.2 %) demonstrated superior diagnostic power compared to FIB-4 (AUC 0.761, sensitivity 75.0 %, and specificity 76.5 %) and APRI (AUC 0.610, sensitivity 62.5 %, and specificity 76.5 %) (Fig. 3A, Table 5). When diagnosing severe liver fibrosis defined by FIB-4, miR-15a had an AUC of 0.744, with a sensitivity of 86.6 % and a specificity of 53.3 %; miRNA-16 yielded an AUC of 0.747, with a sensitivity of 63.0 % and a specificity of 77.6 %; and the combined miR-15a and miR-16 had an AUC of 0.762, with a sensitivity of 79.5 % and a specificity of 62.0 % (Fig. 3C–Table 5). However, these biomarkers showed no diagnostic value for severe liver fibrosis when stratified by APRI (Fig. 3D–Table 5).

In ROC coves plotted between cirrhosis and non-cirrhosis, the diagnostic performance of miR-15a (AUC = 0.832, sensitivity = 76.5 %, specificity = 79.7 %), miR-16 (AUC = 0.815, sensitivity = 87.2 %, specificity = 59.8 %), and the combined miR-15a and miR-16 (AUC = 0.847, sensitivity = 88.8 %, specificity = 68.8 %) were comparable to that of FIB-4 (AUC = 0.857, sensitivity = 81.0 %, specificity = 76.6 %) (Fig. 3B–Table 5). On the other hand, miR-15a, the combination of miR-15a and miR-16, and FIB-4 were outperformed APRI (AUC = 0.768, sensitivity = 73.7 %, specificity = 71.5 %) (Fig. 3B–Table 5). Furthermore, the combination of miR-15a/16 with FIB-4 exhibited the highest AUC of 0.885, with a sensitivity of 88.8 % and a specificity of 72.7 % (Fig. 3B–Table 5). Including healthy controls in the ROC curve plots enhanced the diagnostic parameters of miR-15a, miR-16, and their combination (Supplementary Fig. 5, Supplementary Table 4).

4. Discussion

The disease burden caused by progressive liver fibrosis and the invasive nature of liver biopsy emphasized the urgent need to develop non-invasive diagnostic tests for evaluating liver fibrosis [1,4]. The current investigation explores the correlation between plasma miR-15a/16 and liver fibrosis, severe liver fibrosis, and cirrhosis in CHB patients. Our findings reveal a negative association between the levels of plasma miR-15a/16 and the severity of liver fibrosis, evidenced by lower plasma miR-15a/16 levels in individuals with severe fibrosis compared to those without severe fibrosis, and lower levels in the cirrhosis group compared to the non-cirrhosis group. Moreover, plasma miR-15a/16 levels exhibited a gradual decline with the advancement of the histological fibrosis stage from S0 to S4. These trends were consistently

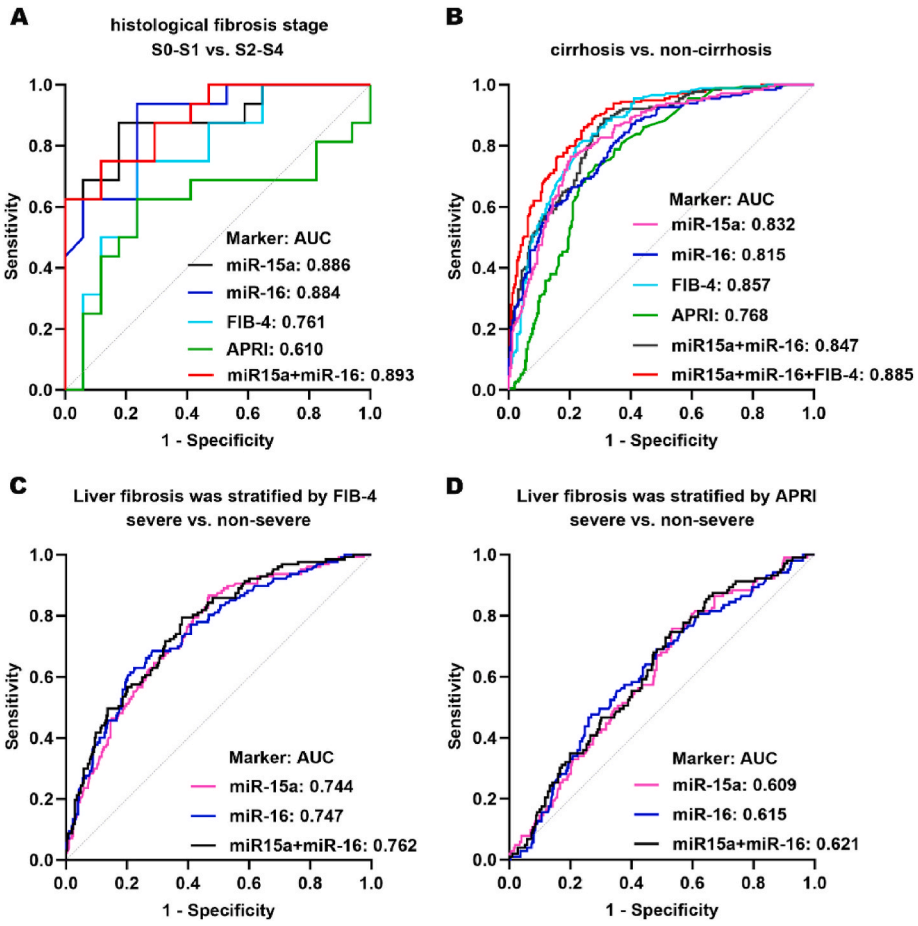

Fig. 3. Performance of plasma miR-15a/16 in detecting moderate-to-severe fibrosis (S2-S4), severe liver fibrosis, and cirrhosis. ROC curves of miR15a, miR16, FIB-4, APRI, and biomarker combinations for diagnosing patients with moderate-to-severe liver fibrosis (S2-S4) (A), patients with cirrhosis (B). The ROC curves of miR15a, miR-16, or their combination in detecting severe liver fibrosis patients under FIB-4 (C) or APRI (D) stratification. FIB-4, fibrosis index based on four factors (incorporating age, aspartate aminotransferase, alanine aminotransferase, and platelet), APRI, aspartate aminotransferase to platelet ratio index. AUC, area under the receiver operating characteristic curve. ROC, receiver operating characteristic.

observed in Pearson's correlation analysis and multivariable linear regressions. Furthermore, multivariable logistic regressions demonstrated that reduced plasma miR-15a/16 levels are linked to an increased prevalence of severe liver fibrosis and cirrhosis, especially within the male subgroup. These findings suggest that measuring plasma miR-15a/16 levels could be a simple and convenient method for assessing liver fibrosis and cirrhosis.

The involvement of miRNAs in liver metabolism, injury, fibrosis, and HCC development emphasizes their significance in liver diseases [24,25]. Hepatic stellate cells (HSCs) activation and phenotypic transformation are significant factors in liver fibrosis development [26]. Microarray analysis has shown a notable decrease in miR-15b/16 levels in activated HSCs [27]. Molecularly, miR-16 modulated the TGF-β and Wnt pathways by targeting genes such as smad2/3, Wnt3a, and lysine oxidase-like 1(LOXL1), which inhibits hepatic stellate cell activation, eliminates the myofibroblastic phenotype, reducing collagen production, and improves liver fibrosis repair [28,29]. Additionally, the miR-15/16 family targets Bcl-2, a key regulator of the mitochondrial apoptosis pathway, thereby inhibiting apoptotic resistance in HSCs through downstream caspases-3/8/9 [27]. Downregulation of miR-16 in HSCs leads to the overexpression of Guanine nucleotide-binding α-subunit 12, which promotes autophagy by coupling with the autophagy-related gene ATG12-5, thereby contributing to liver fibrosis through activating HSCs [15]. The involvement of miR-16 in liver fibrosis may also be related to its participation in the trans-differentiation of HSCs to myofibroblasts [28]. MiR-15a knockdown promoted HSCs activation and proliferation [16]. In summary, miR-15a/16 can regulate the activation of HSCs by integrating signaling pathways such as TGF-β, mitochondrial apoptosis, and cell autophagy, thereby affecting the progression of liver fibrosis. On the other hand, previous studies have reported that HBV components [13,14,30], non-coding RNAs [31,32], and chromosome deletion [33,34] were partly account for the decrease of miR-15a/16. These factors may also contribute to the gradual downregulation of plasma miR-15a and miR-16 observed in the progression of liver fibrosis. Besides, studies have indicated that miR-15a/16 can attenuate fibrosis in peritoneal mesothelial cells and skin fibrosis [35,36]. And miR-15a has been linked to fibroblast activation and lung fibrosis [37]. Collectively, these investigations highlight a close relationship between miR-15a/16 and various forms of organ or tissue fibrosis, particularly liver fibrosis, which supports the results of our study.

Cellular miRNAs can be released into circulation through passive release, lipoprotein complexes, or nanoparticles termed extracellular vesicles, particularly exosomes [18]. Therefore, circulating miRNAs may provide valuable information about the disease and serve as promising diagnostic markers for early-stage, pre-symptomatic patients. Our study found that decreased plasma levels of miR-15a and miR-16 were correlated with an elevated prevalence of severe liver fibrosis and cirrhosis, indicating their diagnostic potential for these conditions. When detecting moderate-to-severe fibrosis (S2-S4), miR-15a, miR-16, and their combination exhibited superior diagnostic performance compared to FIB-4 and APRI. Notably, the combination of miR-15a with

Table 5
Diagnostic power of the indicated variables in detecting moderate-to-severe fibrosis (S2-S4), severe liver fibrosis, and cirrhosis.

Variables	AUC (95 % CI)	Sensitivity (%)	Specificity (%)	*P* value[a]
histological fibrosis stage S0-S1 vs. S2-S4				
miR-15a	0.886 (0.770, 1.000)	87.5	82.4	0.0002
miR-16	0.884 (0.772, 0.996)	93.8	76.5	0.0002
FIB-4	0.761 (0.594, 0.928)	75.0	76.5	0.0105
APRI	0.610 (0.402, 0.819)	62.5	76.5	0.2798
miR-15a + miR-16	0.893 (0.789, 0.998)	75.0	88.2	0.0001
cirrhosis vs. non-cirrhosis				
miR-15a	0.832 (0.794, 0.870)	76.5	79.7	<0.0001
miR-16	0.815 (0.776, 0.855)	87.2	59.8	<0.0001
FIB-4	0.857 (0.822, 0.891)	81.0	76.6	<0.0001
APRI	0.768 (0.724, 0.812)	73.7	71.5	<0.0001
miR-15a + miR-16	0.847 (0.811, 0.883)	88.8	68.8	<0.0001
miR-15a + miR-16 + FIB-4	0.885 (0.855, 0.916)	88.8	72.7	<0.0001
severe vs. non-severe (liver fibrosis was stratified by FIB-4)				
miR-15a	0.744 (0.695, 0.793)	86.6	53.3	<0.0001
miR-16	0.747 (0.696, 0.797)	63.0	77.6	<0.0001
miR-15a + miR-16	0.762 (0.714, 0.809)	79.5	62.0	<0.0001
severe vs. non-severe (liver fibrosis was stratified by APRI)				
miR-15a	0.609 (0.550, 0.669)	75.7	46.7	0.0008
miR-16	0.615 (0.555, 0.676)	47.6	73.2	0.0004
miR-15a + miR-16	0.621 (0.562, 0.680)	74.8	47.3	0.0002

AUC, area under the receiver operating characteristic curve; CI, confidence intervals; FIB-4, fibrosis index based on four factors (incorporating age, aspartate aminotransferase, alanine aminotransferase, and platelet); APRI, aspartate aminotransferase to platelet ratio index.
[a] Null hypothesis: true area = 0.5.

miR-16 yielded an AUC of 0.893, demonstrating higher accuracy than the reported liver fibrosis-associated miRNA-122 (AUC 0.61) and a miRNA-122-based model (AUC 0.85) [38,39]. Furthermore, miR-15a/16 demonstrated diagnostic efficacy for severe liver fibrosis as defined by FIB-4. In distinguishing cirrhosis, the ROC analysis showed that miR-15a/16 was as valuable as FIB-4 and significantly superior to APRI. Noteworthy, the combination of miR-15a/16 with FIB-4 exhibited significantly superior diagnostic performance compared to other markers in this study, achieving an AUC of 0.885. This performance surpasses the accuracy of the reported 'Complex' biomarker blood tests such as Fibrotest/Fibrosure (comprising age, sex, bilirubin, γ-glutamyltransferase, α2-macroglobulin, haptoglobin, and apolipoprotein-A1) and FibroMeter^{v2G} (comprising age, sex, platelets, ALT, AST, γ-glutamyltransferase, prothrombin index, urea, and α2-macroglobulin), which have AUCs ranging from 0.80 to 0.84 [40]. Given the routine application of plasma miRNA detection techniques in clinical settings, measuring plasma levels of miR-15a/16 for monitoring liver fibrosis holds promise for clinical implementation.

It should be noted that the number of patients who underwent liver biopsy in the present study was relatively small. Furthermore, the involvement of plasma miR-15a/16 in liver fibrosis may extend beyond HBV as the primary etiology. Thus, we look forward to evaluating plasma miR-15a/16 as an indicator for liver fibrosis assessment across different primary etiologies. Ideally, a larger longitudinal cohort encompassing a variety of patient types would be preferable to further validate the results of our study.

5. Conclusion

Our study demonstrated that plasma miR-15a/16 is independently correlated with liver fibrosis in CHB patients and may serve as a new indicator for assessing liver fibrosis and predicting severe fibrosis and cirrhosis. Future studies will be needed to monitor plasma miR-15a/16 levels in patients during liver disease development and progression using multicenter, prospective, and longitudinal samples.

Funding

This study was supported by Natural Science Foundation of Guangdong Province (grant number: 2024A1515013208), Guangdong Basic and Applied Basic Research Foundation (grant number: 2023A1515220089), and General Planned Project of Guangzhou Science and Technology (grant numbers: 202201010950 and 202201020422).

Data availability statement

The data of this study can be obtained by contacting the corresponding author. Privacy or ethical restrictions prevent the public availability of the data.

CRediT authorship contribution statement

Huan Wei: Writing – review & editing, Writing – original draft, Visualization, Methodology, Investigation, Data curation. **Yanhua Bi:** Writing – original draft, Validation, Investigation, Funding acquisition, Data curation. **Chunhong Liao:** Investigation, Data curation. **Yuehua Huang:** Writing – review & editing, Supervision, Resources, Project administration, Conceptualization. **Yifan Lian:** Writing – review & editing, Supervision, Resources, Project administration, Funding acquisition, Formal analysis, Conceptualization.

Declaration of competing interest

The authors declare that none of the authors had a conflict of interest.

Appendix A. Supplementary data

Supplementary data to this article can be found online at https://doi.org/10.1016/j.ncrna.2024.08.004.

References

[1] P. Gines, A. Krag, J.G. Abraldes, E. Sola, N. Fabrellas, P.S. Kamath, Liver cirrhosis, Lancet 398 (2021) 1359–1376, https://doi.org/10.1016/S0140-6736(21)01374-X.
[2] S.L. Friedman, M. Pinzani, Hepatic fibrosis 2022: unmet needs and a blueprint for the future, Hepatology 75 (2022) 473–488, https://doi.org/10.1002/hep.32285.
[3] N.A. Terrault, A.S.F. Lok, B.J. McMahon, K.M. Chang, J.P. Hwang, M.M. Jonas, et al., Update on prevention, diagnosis, and treatment of chronic hepatitis B: AASLD 2018 hepatitis B guidance, Hepatology 67 (2018) 1560–1599, https://doi.org/10.1002/hep.29800.
[4] A. Regev, M. Berho, L.J. Jeffers, C. Milikowski, E.G. Molina, N.T. Pyrsopoulos, et al., Sampling error and intraobserver variation in liver biopsy in patients with chronic HCV infection, Am. J. Gastroenterol. 97 (2002) 2614–2618, https://doi.org/10.1111/j.1572-0241.2002.06038.x.
[5] J.A. Udell, C.S. Wang, J. Tinmouth, J.M. FitzGerald, N.T. Ayas, D.L. Simel, et al., Does this patient with liver disease have cirrhosis? JAMA 307 (2012) 832–842, https://doi.org/10.1001/jama.2012.186.
[6] J. Zheng, H. Guo, J. Zeng, Z. Huang, B. Zheng, J. Ren, et al., Two-dimensional shear-wave elastography and conventional US: the optimal evaluation of liver fibrosis and cirrhosis, Radiology 275 (2015) 290–300, https://doi.org/10.1148/radiol.14140828.

[7] L. European Association for Study of, H, Asociacion Latinoamericana para el Estudio del. EASL-ALEH Clinical Practice Guidelines: Non-invasive tests for evaluation of liver disease severity and prognosis, J. Hepatol. 63 (2015) 237–264, https://doi.org/10.1016/j.jhep.2015.04.006.
[8] S. Singh, A.J. Muir, D.T. Dieterich, Y.T. Falck-Ytter, American gastroenterological association Institute technical review on the role of elastography in chronic liver diseases, Gastroenterology 152 (2017) 1544–1577, https://doi.org/10.1053/j.gastro.2017.03.016.
[9] K. Imajo, Y. Honda, T. Kobayashi, K. Nagai, A. Ozaki, M. Iwaki, et al., Direct comparison of US and MR elastography for staging liver fibrosis in patients with nonalcoholic fatty liver disease, Clin. Gastroenterol. Hepatol. 20 (2022) 908–917 e911, https://doi.org/10.1016/j.cgh.2020.12.016.
[10] D.P. Bartel, MicroRNAs: genomics, biogenesis, mechanism, and function, Cell 116 (2004) 281–297, https://doi.org/10.1016/s0092-8674(04)00045-5.
[11] E. Huang, R. Liu, Y. Chu, miRNA-15a/16: as tumor suppressors and more, Future Oncol. 11 (2015) 2351–2363, https://doi.org/10.2217/fon.15.101.
[12] Y.F. Lian, Y.L. Huang, J.L. Wang, M.H. Deng, T.L. Xia, M.S. Zeng, et al., Anillin is required for tumor growth and regulated by miR-15a/miR-16-1 in HBV-related hepatocellular carcinoma, Aging (Albany N Y) 10 (2018) 1884–1901, https://doi.org/10.18632/aging.101510.
[13] G. Wu, F. Yu, Z. Xiao, K. Xu, J. Xu, W. Tang, et al., Hepatitis B virus X protein downregulates expression of the miR-16 family in malignant hepatocytes in vitro, Br. J. Cancer 105 (2011) 146–153, https://doi.org/10.1038/bjc.2011.190.
[14] N. Liu, J. Zhang, T. Jiao, Z. Li, J. Peng, Z. Cui, et al., Hepatitis B virus inhibits apoptosis of hepatoma cells by sponging the MicroRNA 15a/16 cluster, J. Virol. 87 (2013) 13370–13378, https://doi.org/10.1128/JVI.02130-13.
[15] K.M. Kim, C.Y. Han, J.Y. Kim, S.S. Cho, Y.S. Kim, J.H. Koo, et al., Galpha12 overexpression induced by miR-16 dysregulation contributes to liver fibrosis by promoting autophagy in hepatic stellate cells, J. Hepatol. 68 (2018) 493–504, https://doi.org/10.1016/j.jhep.2017.10.011.
[16] M. Fu, W. Yin, W. Zhang, Y. Zhu, H. Ni, L. Gong, MicroRNA-15a inhibits hepatic stellate cell activation and proliferation via targeting SRY-box transcription factor 9, Bioengineered 13 (2022) 13011–13020, https://doi.org/10.1080/21655979.2022.2068895.
[17] J. Tak, Y.S. Kim, T.H. Kim, G.C. Park, S. Hwang, S.G. Kim, Galpha12 overexpression in hepatocytes by ER stress exacerbates acute liver injury via ROCK1-mediated miR-15a and ALOX12 dysregulation, Theranostics 12 (2022) 1570–1588, https://doi.org/10.7150/thno.67722.
[18] A.E. do Amaral, J. Cisilotto, T.B. Creczynski-Pasa, L. de Lucca Schiavon, Circulating miRNAs in nontumoral liver diseases, Pharmacol. Res. 128 (2018) 274–287, https://doi.org/10.1016/j.phrs.2017.10.002.
[19] H. Wei, S. Luo, Y. Bi, C. Liao, Y. Lian, J. Zhang, et al., Plasma microRNA-15a/16-1-based machine learning for early detection of hepatitis B virus-related hepatocellular carcinoma, Liver Res. (2024), https://doi.org/10.1016/j.livres.2024.05.003.
[20] C.T. Wai, J.K. Greenson, R.J. Fontana, J.D. Kalbfleisch, J.A. Marrero, H. S. Conjeevaram, et al., A simple noninvasive index can predict both significant fibrosis and cirrhosis in patients with chronic hepatitis C, Hepatology 38 (2003) 518–526, https://doi.org/10.1053/jhep.2003.50346.
[21] R.K. Sterling, E. Lissen, N. Clumeck, R. Sola, M.C. Correa, J. Montaner, et al., Development of a simple noninvasive index to predict significant fibrosis in patients with HIV/HCV coinfection, Hepatology 43 (2006) 1317–1325, https://doi.org/10.1002/hep.21178.
[22] H. Yoshiji, S. Nagoshi, T. Akahane, Y. Asaoka, Y. Ueno, K. Ogawa, et al., Evidence-based clinical practice guidelines for Liver Cirrhosis 2020, J. Gastroenterol. 56 (2021) 593–619, https://doi.org/10.1007/s00535-021-01788-x.
[23] I. Balcells, S. Cirera, P.K. Busk, Specific and sensitive quantitative RT-PCR of miRNAs with DNA primers, BMC Biotechnol. 11 (2011) 70, https://doi.org/10.1186/1472-6750-11-70.
[24] X.W. Wang, N.H. Heegaard, H. Orum, MicroRNAs in liver disease, Gastroenterology 142 (2012) 1431–1443, https://doi.org/10.1053/j.gastro.2012.04.007.
[25] M. Gjorgjieva, C. Sobolewski, D. Dolicka, M. Correia de Sousa, M. Foti, miRNAs and NAFLD: from pathophysiology to therapy, Gut 68 (2019) 2065–2079, https://doi.org/10.1136/gutjnl-2018-318146.
[26] S.L. Friedman, Mechanisms of hepatic fibrogenesis, Gastroenterology 134 (2008) 1655–1669, https://doi.org/10.1053/j.gastro.2008.03.003.
[27] C.J. Guo, Q. Pan, D.G. Li, H. Sun, B.W. Liu, miR-15b and miR-16 are implicated in activation of the rat hepatic stellate cell: an essential role for apoptosis, J. Hepatol. 50 (2009) 766–778, https://doi.org/10.1016/j.jhep.2008.11.025.
[28] Q. Pan, C.J. Guo, Q.Y. Xu, J.Z. Wang, H. Li, C.H. Fang, miR-16 integrates signal pathways in myofibroblasts: determinant of cell fate necessary for fibrosis resolution, Cell Death Dis. 11 (2020) 639, https://doi.org/10.1038/s41419-020-02832-z.
[29] L. Ma, J. Liu, E. Xiao, H. Ning, K. Li, J. Shang, et al., MiR-15b and miR-16 suppress TGF-beta1-induced proliferation and fibrogenesis by regulating LOXL1 in hepatic stellate cells, Life Sci. 270 (2021) 119144, https://doi.org/10.1016/j.lfs.2021.119144.
[30] Y. Wang, L. Jiang, X. Ji, B. Yang, Y. Zhang, X.D. Fu, Hepatitis B viral RNA directly mediates down-regulation of the tumor suppressor microRNA miR-15a/miR-16-1 in hepatocytes, J. Biol. Chem. 288 (2013) 18484–18493, https://doi.org/10.1074/jbc.M113.458158.
[31] C.R. Xie, F. Wang, S. Zhang, F.Q. Wang, S. Zheng, Z. Li, et al., Long noncoding RNA HCAL facilitates the growth and metastasis of hepatocellular carcinoma by acting as a ceRNA of LAPTM4B, Mol. Ther. Nucleic Acids 9 (2017) 440–451, https://doi.org/10.1016/j.omtn.2017.10.018.
[32] Y. He, H. Huang, L. Jin, F. Zhang, M. Zeng, L. Wei, et al., CircZNF609 enhances hepatocellular carcinoma cell proliferation, metastasis, and stemness by activating the Hedgehog pathway through the regulation of miR-15a-5p/15b-5p and GLI2 expressions, Cell Death Dis. 11 (2020) 358, https://doi.org/10.1038/s41419-020-2441-0.
[33] G.A. Calin, C.D. Dumitru, M. Shimizu, R. Bichi, S. Zupo, E. Noch, et al., Frequent deletions and down-regulation of micro- RNA genes miR15 and miR16 at 13q14 in chronic lymphocytic leukemia, Proc. Natl. Acad. Sci. U. S. A. 99 (2002) 15524–15529, https://doi.org/10.1073/pnas.242606799.
[34] B. Skawran, D. Steinemann, T. Becker, R. Buurman, J. Flik, B. Wiese, et al., Loss of 13q is associated with genes involved in cell cycle and proliferation in dedifferentiated hepatocellular carcinoma, Mod. Pathol. 21 (2008) 1479–1489, https://doi.org/10.1038/modpathol.2008.147.
[35] J. Shang, Q. He, Y. Chen, D. Yu, L. Sun, G. Cheng, et al., miR-15a-5p suppresses inflammation and fibrosis of peritoneal mesothelial cells induced by peritoneal dialysis via targeting VEGFA, J. Cell. Physiol. 234 (2019) 9746–9755, https://doi.org/10.1002/jcp.27660.
[36] Y. Bo, B. Liu, L. Yang, L. Zhang, Y. Yan, Exosomes derived from miR-16-5p-overexpressing keratinocytes attenuates bleomycin-induced skin fibrosis, Biochem. Biophys. Res. Commun. 561 (2021) 113–119, https://doi.org/10.1016/j.bbrc.2021.05.046.
[37] Y. Chen, X. Zhao, J. Sun, W. Su, L. Zhang, Y. Li, et al., YAP1/Twist promotes fibroblast activation and lung fibrosis that conferred by miR-15a loss in IPF, Cell Death Differ. 26 (2019) 1832–1844, https://doi.org/10.1038/s41418-018-0250-0.
[38] C.J. Pirola, T. Fernandez Gianotti, G.O. Castano, P. Mallardi, J. San Martino, M. Mora Gonzalez Lopez Ledesma, et al., Circulating microRNA signature in non-alcoholic fatty liver disease: from serum non-coding RNAs to liver histology and disease pathogenesis, Gut 64 (2015) 800–812, https://doi.org/10.1136/gutjnl-2014-306996.
[39] K. Appourchaux, S. Dokmak, M. Resche-Rigon, X. Treton, M. Lapalus, C. H. Gattolliat, et al., MicroRNA-based diagnostic tools for advanced fibrosis and cirrhosis in patients with chronic hepatitis B and C, Sci. Rep. 6 (2016) 34935, https://doi.org/10.1038/srep34935.
[40] R. Loomba, L.A. Adams, Advances in non-invasive assessment of hepatic fibrosis, Gut 69 (2020) 1343–1352, https://doi.org/10.1136/gutjnl-2018-317593.